https://russjcardiol.elpub.ru
doi:10.15829/1560-4071-2020-3739

ISSN 1560-4071 (print)
ISSN 2618-7620 (online)

Chaotic global analysis of heart rate variability following power spectral adjustments during exposure to traffic noise in healthy adult women

Garner D. M.[1,2], Alves M.[2], da Silva B. P.[2], de Alcantara Sousa L. V.[3], Valenti V. E.[2]

Aim. Previous studies have described the substantial impact of different types of noise on the linear behaviour of heart rate variability (HRV). Yet, there are limited studies about the complexity or nonlinear dynamics of HRV during exposure to traffic noise. Here, we evaluated the complexity of HRV during traffic noise exposure via six power spectra and, when adjusted by the parameters of the Multi-Taper Method (MTM).

Material and methods. We analysed 31 healthy female students between 18 and 30 years old. Subjects remained at rest, seated under spontaneous breathing for 20 minutes with an earphone turned off and then the volunteers were exposed to traffic noise through an earphone for a period of 20 minutes. The traffic noise was recorded from a busy urban street and the sound involved car, bus, trucks engineers and horn sounds (71-104 dB).

Results. The results stipulate that CFP3 and CFP6 are the best metrics to distinguish the two groups. The most appropriate power spectra were, Welch and MTM. Increasing the DPSS parameter of MTM increased the performance of both CFP3 and CFP6 as mathematical markers. Adaptive was the preferred type for Thomson's nonlinear combination method.

Conclusion. CFP3 with the adaptive option for MTM, and increased DPSS is designated as the best mathematical marker on the basis of five statistical tests.

Key words: autonomic nervous system, cardiovascular physiology, cardiovascular system, noise, noise occupational, nonlinear dynamics.

Relationships and Activities. This study received financial support from FAPESP (Process number 2012/01366-6). Dr. Vitor E. Valenti receives financial support from the National Council for Scientific and Technological Development, an entity linked to the Ministry of Science, Technology, Innovations and Communications from Brazil (Process number 302197/2018-4).

[1]Cardiorespiratory Research Group, Department of Biological and Medical Sciences, Faculty of Health and Life Sciences, Oxford Brookes University, Headington Campus, Oxford, United Kingdom; [2]Autonomic Nervous System Center, Sao Paulo State University, Marília, Brazil; [3]School of Medicine of ABC, Santo Andre, Brazil.

Garner D. M.* — PhD candidate, ORCID: 0000-0002-8114-9055, Alves M. — PT, ORCID: 0000-0001-8846-1626, da Silva B. P. — M. Sc. candidate, ORCID: 0000-0002-0570-8345, de Alcantara Sousa L. V. — PhD, Assistant Professor, ORCID: 0000-0002-6895-4914, Valenti V. E. — PhD, Adjunct Professor, ORCID: 0000-0001-7477-3805.

*Corresponding author:
davidmgarner1@gmail.com

Received: 05.02.2020
Revision Received: 29.02.2020
Accepted: 09.03.2020

For citation: Garner D. M., Alves M., da Silva B. P., de Alcantara Sousa L. V., Valenti V. E. Chaotic global analysis of heart rate variability following power spectral adjustments during exposure to traffic noise in healthy adult women. *Russian Journal of Cardiology*. 2020;25(6):3739. doi:10.15829/1560-4071-2020-3739

Traffic noise exposure can be unpleasant and distracting, which may have effects on physiological variables. It is often found in hazardous situations as a result of industrialization and urbanization [1]. Hence, the scientific research literature has previously investigated the effects of different types of noise on autonomic nervous system (ANS) by investigating heart rate variability (HRV) [1].

The consecutive heart beats (RR-intervals) derived from the electrocardiograph (ECG) have been demonstrated to fluctuate in an irregular and chaotic manner [2]. Here, the objective is to estimate the possible pathological risks that traffic noise exposure during driving in women poses to the individual by evaluating the heart rate variability (HRV). To complete this we enforced the Shannon Entropy [3] and Detrended Fluctuation Analysis (DFA) [4] algorithms to six alternate power spectra to understand which exhibited the greatest parametric sensitivity. At the outset, Garner and Ling [5] computed the spectral Entropy 5and spectral Detrended Fluctuation Analysis (sDFA) [5], and these were based on the Welch power spectrum [6, 7]. Later, the *high spectral* Entropy (*hs*Entropy) [8] and *high spectral* Detrended Fluctuation Analysis (*hs*DFA) [8]; were formulated founded on the Multi-Taper Method (MTM) power spectrum [9]. Yet, here further parameters based on Covariance [10], Burg [10], Yule-Walker [11] and the Periodogram [12] are computed. By implementing six different power spectra we hope to accomplish results of greater significance by parametric and non-parametric statistics and, the three effect sizes (discussed later) when equating the control subjects to those experiencing exposure to traffic noise via an earphone. It would then be possible to reach a clinical diagnosis quicker and provide the required treatment earlier.

Chaotic global techniques are more responsive to erraticism in dynamical systems than those based on linear, time-domain, geometric methods, frequency domain or the nonlinear measurements [2]. Chaotic behaviour in biological systems typically indicates normal physiological status; while a reduction of chaotic tendencies could be a pathophysiological marker [13]. Such computations are beneficial when assessing surgical patients [13], particularly if sedated [14, 15] or incapable of indicating discomfort as with sleep apnea [16] or those with "air hunger" [17, 18]. We expected the subjects exposed to traffic noise to perform in a nonlinear manner equivalent to persons with cardiac arrest [19], epileptic seizures [20, 21], chronic obstructive pulmonary disease (COPD) [22] or attention deficit hyperactivity disorder (ADHD) [8].

The advantage for constructing the correlation with HRV is that it can provide a benchmark of the potential risks of the dynamical diseases [23] in the traffic noise exposure group. HRV is a simple, reliable and inexpensive technique to continuously record the ANS. Therefore, we aimed to evaluate nonlinear HRV through chaotic global analysis during exposure to traffic noise.

Material and methods

All method and materials were exactly as in the study by Alves M, et al. [24], which followed the STROBE (STrengthening the Reporting of OBservational studies in Epidemiology) guidelines. Our study previously published [24] described information regarding setting, variables, study design, participants, measurements, data sources, quantitative variables description, statistical methods and potential sources of bias.

Ethical approval and informed consent. All procedures were performed in accordance with the 466/2012 resolution of the National Health Council of December 12th 2012 and all subjects signed a confidential informed consent letter. All experimental protocols were inspected and approved by the Research Ethics Committee in Research of UNESP/Marilia through the Brazilian online platform (Number 5406).

Six Power Spectra. Formerly, we computed the Welch and Multi-Taper Method (MTM) power spectras. De Souza NM, et al. [25] described the application of the Welch power spectrum to achieve chaotic globals in subjects with type I diabetes mellitus. Yet, it was anticipated that since the MTM is an adaptive and nonlinear technique, and as such has a reduced amount of spectral leakage it would potentially be more sensitive to chaotic responses. The *high spectral* Entropy (*hs*Entropy) and *high spectral* Detrended Fluctuation Analysis (*hs*DFA) via the MTM power spectrum have been applied in studies on malnutrition [26], youth obesity [27] and ADHD [8]. Throughout all of the studies we applied the MTM power spectrum to generate the third parameter spectral Multi-Taper Method (sMTM) [5]. This quantifies the extent of broadband noise in the system associated with increasing chaotic response. This parameter remains unchanged throughout all the subsequent analysis.

In this study, when calculating spectral Entropy (*hs*Entropy for MTM) or spectral DFA (*hs*DFA for MTM) we enforce six different power spectra (Welch, MTM, Covariance, Burg, Yule-Walker and Periodogram) to give six variants of these parameters. There are seven different non-trivial permutations of three chaotic globals. The Chaotic Forward Parameters (CFP1 to CFP7) enables seven different combinations of chaotic globals to be applied to ensure optimum chaotic response. Initially whilst assessing the

effects of the six power spectra all three chaotic global values have equal weighting of unity. The settings for these six power spectra are described next.

When we compute spectral Entropy and sDFA via Welch's method the parameters are set at: (i) sampling frequency of 1Hz, (ii) 50% overlap, (iii) a Hamming window and the number of discrete Fourier transform (DFT) point to use in the power spectral density (PSD) estimate is the greater of 256 or the next power of two greater than the length of the segments, and (iv) there is no detrending.

Then, with MTM, the parameters are set as the following: (i) sampling frequency of 1Hz; (ii) time bandwidth for the discrete prolate spheroidal sequences (DPSS) often referred to as slepian sequences [28] is 3; (iii) FFT is the larger of 256 and the next power of two greater than the length of the segment (iv) Thomson's adaptive nonlinear combination method to combine individual spectral estimates is applied.

The Periodogram power spectral density estimate is a nonparametric estimate of a wide-sense stationary random process using a rectangular window. The number of points in the discrete Fourier transform (DFT) is a maximum of 256 or the next power of two greater than the signal length.

Finally, for the Covariance, Burg and Yule-Walker methods the order is of the autoregressive model (AR) used to produce the power spectra density estimate and is set to 16. A default discrete Fourier transform (DFT) length of 256 is applied.

Nonlinear & statistical analysis

Chaotic Globals & CFP1 to CFP7. Spectral Entropy [5] (*hs*Entropy for the MTM) is an algorithm founded on the unevenness of the amplitude and frequency of the power spectrums peaks. Shannon entropy [3] is the function applied to the cited power spectrum. We compute the Shannon entropy for three values attained from three various power spectra. So, the power spectra at three test settings: (a) a sine wave, (b) uniformly distributed random variables, and (c) the oscillating signal from the subjects exposed to traffic noise. The three values are reduced proportionately so that their sum of squares is equal to one. Spectral Entropy (*hs*Entropy for the MTM) is the median value of the three.

DFA was derived in 1995 [4]. It can be executed on time-series where the mean, variance and autocorrelation adjust with time. sDFA (or, *hs*DFA for MTM) is where DFA is applied to the frequency rather than time. To acquire sDFA (or, *hs*DFA for MTM) we estimate the spectral adaptation in precisely the same manner as with Spectral Entropy (or, *hs*Entropy for MTM). Yet, DFA is the algorithm enforced onto the appropriate power spectrum.

Spectral Multi-Taper Method (sMTM) [5] is derived from elevated broadband noise intensities generated in MTM power spectra by irregular and often chaotic signals. sMTM is the area beneath the power spectrum but above the baseline.

CFP1 to CFP7 are applied to RR-intervals from the control subjects and those undergoing traffic noise exposure. sDFA (and *hs*DFA) respond to chaos contrariwise to the others, so we subtract its value from unity. There are seven non-trivial permutations of the three chaotic globals [8].

One-Way Analysis Of Variance & Kruskal-Wallis Tests. Parametric statistics accept that datasets are normally distributed, so they use the mean as a measure of central tendancy. If we are unable to normalize the data we should not compare means. To prove normality we assessed the Anderson-Darling [29], Ryan-Joiner [30] and Lilliefors [29] tests. The Anderson-Darling test for normality applies an empirical cumulative distribution function, but the Ryan-Joiner test is a correlation-based test comparable to Shapiro-Wilk [31]. The Lilliefors test is particularly useful when studies have small sample sizes. Yet, in this study results were inconclusive throughout so we cannot declare that the observations are normally or non-normally distributed. So, we apply parametric and non-parametric tests of significance. Those chosen were the one-way analysis of variance (ANOVA1) [32] and the Kruskal-Wallis [33] tests of significance, respectively.

Cohen's d_s, Hedges's g_s and Glass's Δ Tests. Cohen's d_s [34] is the leading subcategory of effect sizes. It refers to the standardized mean difference between two groups of independent observations for the appropriate sample [35]. It is founded on the sample means and gives a *biased* estimate of the population effect size [36].

In the algebraic formula for Cohen's d_s, the numerator is the variation between the means of two groups of observations. The denominator is the pooled standard deviation. These differences are squared. Then, they are summed and divided by the number of observations minus one for bias (hence, *Bessel's correction*) in the estimate of the population variance. Finally, the square root is applied.

$$Cohen's\ d_s = \frac{\overline{X}_1 - \overline{X}_2}{\sqrt{\frac{(n_1-1)SD_1^2 + (n_2-1)SD_2^2}{n_1+n_2-2}}}$$

Cohen's d_s is often denoted as the *uncorrected* effect size. The *corrected* effect size is *unbiased* and may be termed Hedges's g_s [37]. The difference between Cohen's d_s and Hedges's g_s is tiny especially in sample sizes greater than 20 [38]. Its algebraic formula is beneath. The same subscript letter in Hed-

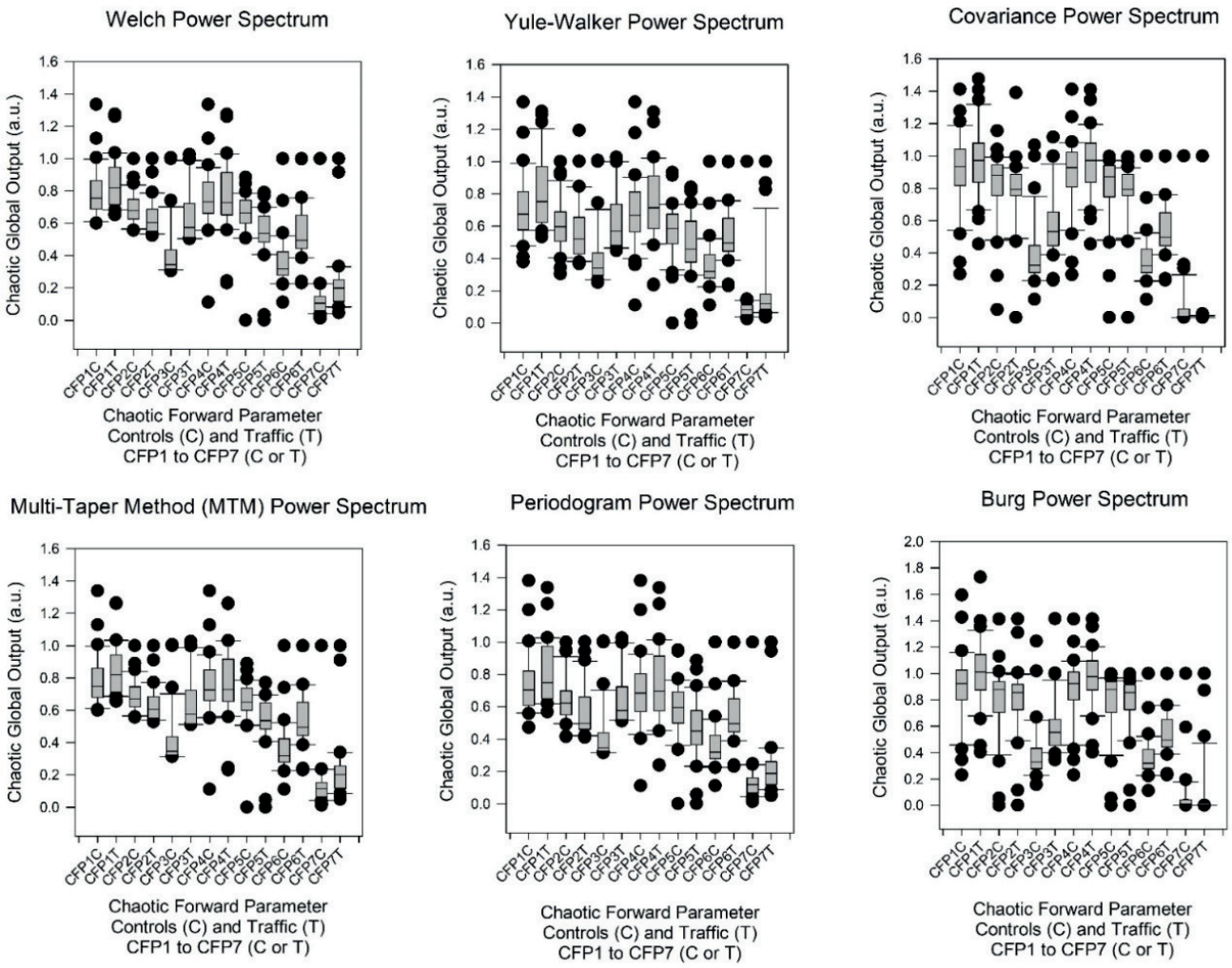

Figure 1. The boxplots of the seven combinations of chaotic forward parameters (CFP 1 to 7) for the six power spectra density (PSD) estimates (Welch, MTM, Burg, Covariance, Yule-Walker and Periodogram) of 500 RR intervals in control subjects (CFPx C) and traffic noise exposed subjects (CFPx T).

Note: the point closest to the zero is the minimum and the point farthest away is the maximum. The point next closest to the zero is the 5th percentile and the point next farthest away is the 95th percentile. The boundary of the box closest to zero indicates the 25th percentile, a line within the box marks the median (not the mean), and the boundary of the box farthest from zero indicates the 75th percentile. The difference between these points is the inter-quartile range (IQR). Whiskers (or error bars) above and below the box indicate the 90th and 10th percentiles respectively.

ges's g_s is applied to distinguish the different calculations; as is the case here for Cohen's d_s.

$$Hedges's\ g_s = Cohen's\ d_s \times \left[1 - \frac{3}{4(n_1+n_2)-9}\right]$$

Finally, when the standard deviations differ substantially between conditions, Glass's Δ delta may be suitable [39]. This calculates the control group's standard deviation alone, and the experimental group is avoided.

For all effects' sizes but particularly with Cohen's d_s the extents are nominated as 0,01> very small effect; 0,20> small effect; 0,50> medium effect; 0,80> large effect; 1,20> very large effect; 2,00> huge effect. These are based on the standards provided by Cohen [34] and, Sawilowsky [40].

CFP3 & CFP6 — MTM Spectrum only

Thomson's nonlinear combination methods & DPSS. Now we assess the outcome of manipulating Thomson's nonlinear combination settings on the MTM spectra. There are three options. They are "adapt", "eigen", or "unity" and are the weights on individual tapered power spectral density (PSD) estimates. The default "adapt" is the adaptive frequency-dependent weights. The "eigen" method weights each tapered PSD estimate by the eigenvalue (frequency concentration) of the corresponding Slepian taper. The "unity" method weights each tapered PSD estimate equally [41].

Table 1

Chaotic responses (CFP 1 to CFP 7) derived via six power spectra (Welch, MTM, Burg, Covariance, Yule-Walker & Periodogram) for control subjects (n=31) and those undergoing traffic noise exposure (n=31)

Power Spectrum	CFP (1 to 7)	ANOVA1	Kruskal-Wallis	Glass's Δ Delta	Hedges g_s	Cohen's d_s
MTM	CFP1	0,1243	0,0704	0,3982	0,3910	0,3960
	CFP2	0,0395	0,0043	-0,5625	-0,5280	-0,5347
	CFP3	<0,0001	<0,0001	1,2210	1,2720	1,2882
	CFP4	0,5739	0,4182	0,1531	0,1418	0,1436
	CFP5	0,0121	0,0011	-0,6905	-0,6487	-0,6569
	CFP6	<0,0001	<0,0001	1,1530	1,0984	1,1124
	CFP7	0,0748	0,0016	0,5156	0,4548	0,4606
Burg	CFP1	0,1291	0,0621	0,3798	0,3860	0,3909
	CFP2	0,9282	0,9047	0,0229	0,0227	0,0230
	CFP3	0,0007	<0,0001	0,9064	0,9023	0,9138
	CFP4	0,1105	0,0727	0,3921	0,4063	0,4115
	CFP5	0,9506	0,7039	-0,0153	-0,0156	-0,0158
	CFP6	<0,0001	<0,0001	1,1530	1,0984	1,1124
	CFP7	0,7956	0,0911	0,0737	0,0653	0,0661
Welch	CFP1	0,1410	0,0981	0,3846	0,3741	0,3789
	CFP2	0,0321	0,0045	-0,5955	-0,5503	-0,5572
	CFP3	<0,0001	<0,0001	1,2163	1,2649	1,2810
	CFP4	0,6067	0,5310	0,1409	0,1298	0,1315
	CFP5	0,0108	0,0013	-0,7091	-0,6599	-0,6683
	CFP6	<0,0001	<0,0001	1,1530	1,0984	1,1124
	CFP7	0,0745	0,0013	0,5177	0,4552	0,4610
Yule-Walker	CFP1	0,0927	0,0898	0,4429	0,4285	0,4340
	CFP2	0,3877	0,1699	-0,2478	-0,2182	-0,2210
	CFP3	<0,0001	<0,0001	1,2084	1,2130	1,2285
	CFP4	0,3343	0,2752	0,2540	0,2441	0,2472
	CFP5	0,0659	0,0412	-0,4878	-0,4698	-0,4758
	CFP6	<0,0001	<0,0001	1,1530	1,0984	1,1124
	CFP7	0,1050	0,0021	0,5142	0,4129	0,4181
Periodogram	CFP1	0,1769	0,1571	0,3473	0,3427	0,3471
	CFP2	0,0915	0,0152	-0,4715	-0,4302	-0,4356
	CFP3	<0,0001	<0,0001	1,2312	1,2754	1,2916
	CFP4	0,5996	0,5590	0,1402	0,1324	0,1341
	CFP5	0,0118	0,0041	-0,6958	-0,6517	-0,6600
	CFP6	<0,0001	<0,0001	1,1530	1,0984	1,1124
	CFP7	0,0757	0,0022	0,5194	0,4533	0,4591
Covariance	CFP1	0,2100	0,2233	0,3085	0,3178	0,3219
	CFP2	0,6217	0,1165	-0,1238	-0,1244	-0,1260
	CFP3	0,0012	<0,0001	0,8479	0,8558	0,8666
	CFP4	0,1417	0,1132	0,3520	0,3735	0,3782
	CFP5	0,7448	0,2370	-0,0771	-0,0820	-0,0831
	CFP6	<0,0001	<0,0001	1,1530	1,0984	1,1124
	CFP7	0,4265	0,0060	-0,1980	-0,2008	-0,2033

Note: table of results for the chaotic responses (CFP 1 to CFP 7) derived via six power spectra (Welch, MTM, Burg, Covariance, Yule-Walker & Periodogram) for those control subjects (n=31) and those undergoing traffic noise exposure (n=31). We computed the significance (p-value) by parametric and nonparametric techniques: One way Analysis of Variance (ANOVA1) and Kruskal-Wallis tests of significance, respectively. We also calculated the effect sizes Glass's Δ Delta, Hedges g_s and Cohen's d_s. We assessed 500 RR-intervals throughout.

Table 2

The properties of the discrete prolate spheroidal sequences (DPSS) value (2 to 13) on the effect sizes Glass's Δ Delta, Hedges g_s and Cohen's d_s

DPSS Value	CFP3 *adaptive*			CFP6 *adaptive*		
	Glass's Δ delta	Hedge's g_s	Cohen's d_s	Glass's Δ delta	Hedge's g_s	Cohen's d_s
2	1,2101	1,2707	1,2869	1,1366	1,0912	1,1050
3	1,2221	1,2734	1,2896	1,1530	1,0984	1,1124
4	1,2197	1,2709	1,2871	1,1464	1,0943	1,1082
5	1,2324	1,2849	1,3012	1,1580	1,1053	1,1193
6	1,2406	1,2935	1,3099	1,1666	1,1137	1,1278
7	1,2423	1,2950	1,3115	1,1682	1,1149	1,1290
8	1,2442	1,2969	1,3134	1,1706	1,1172	1,1314
9	1,2442	1,2974	1,3139	1,1699	1,1174	1,1316
10	1,2436	1,2969	1,3134	1,1690	1,1168	1,1310
11	1,2440	1,2973	1,3138	1,1692	1,1171	1,1313
12	1,2435	1,2968	1,3133	1,1684	1,1165	1,1307
13	1,2451	1,2984	1,3149	1,1706	1,1183	1,1325

Note: the properties of the discrete prolate spheroidal sequences (DPSS) value (2 to 13) on the effect sizes Glass's Δ Delta, Hedges g_s and Cohen's d_s when comparing chaotic globals CFP3 and CFP6 for control subjects and those undergoing traffic noise exposure (both n=31). The remaining parameters are set as (a) sampling frequency of 1Hz; is (b) a discrete Fourier transform (DFT) length of 256 or the next power of two greater than the length of the segment (c) Thomson's "*adaptive*" nonlinear combination method to combine individual spectral estimates is applied. 500 RR-intervals were assessed thoughout.

Moreover, we simultaneously assess the effect of changing the settings of the DPSS from 2 to 13. A DPSS equal to 1, indicates the conventional Blackman and Tukey [42, 43] Fast Fourier Transform (FFT), so is excluded.

DPSS affects the adaptation properties of the tapers with the intention of reducing spectral leakage. Whilst assessing the outcomes of the Thomson's nonlinear combinations settings and the levels of DPSS on the chaotic response the sampling frequency is fixed at 1Hz for the MTM and Fast Fourier Transform of length 256 is enforced. We assessed the outcomes of DPSS (2 to 13) and Thomson's nonlinear combinations ("adaptive", "eigen" and "unity"). Throughout the analysis there are 500 RR-intervals. We assessed CFP3 and CFP6. These are the only groupings significant under the default conditions and with all six power spectra.

Results

ANOVA1, Kruskal-Wallis & Effect Sizes

We have computed the seven permutations of the three chaotic globals CFP1 to CFP7 for 31 female subjects; both controls and those exposed to traffic noise via the earphone. We achieved this with 500 RR intervals throughout. The statistical results are illustrated in the six boxplots, one for each power spectrum as in Figure 1.

As of Table 1 we detected that the combinations CFP3 and CFP6 behave equally during all six power spectra. All CFP3 and CFP6 for Welch, MTM, Covariance, Burg, Yule-Walker and Periodogram have similar reponses. They have a $p<0,001$ for the ANOVA1 and Kruskal-Wallis tests of significance and, have large to very large effect sizes by all three measures — Glass's Δ Delta, Hedges g_s and Cohen's d_s. They demonstrate an *increase* in chaotic response when comparing the controls to the traffic noise exposed group.

With MTM and Welch power spectra there are also significant results for CFP2 ($p<0,05$, medium effect sizes) and CFP5 ($p<0,01$, large effect sizes). Be that as it may, as revealed by the negative effect sizes the traffic noise exposed subjects exhibit a *decrease* in response when comparing control to the traffic noise exposed subjects. The Welch and MTM power spectra perform similarly throughout. MTM has the slightly better levels of significance when compared by the three effect sizes. It is not possible to distinguish between the two on the basis of the ANOVA1 and Kruskal-Wallis tests as the both give $p<0,001$. This is the advantage of calculating the effect sizes in this study.

Next the Periodogram power spectra has a significant result for CFP5 ($p<0,01$, medium effect size), yet the effect size value is *negative* and so responds in the opposite direction to those it calculated for CFP3 and CFP6. Those values which give negative values for the effect sizes can be ignored. They are responding incorrectly and have the lesser significances than CFP3 and CFP6.

Table 3

The properties of the discrete prolate spheroidal sequences (DPSS) value (2 to 13) on the effect sizes called Glass's Δ Delta, Hedges g_s and Cohen's d_s

DPSS Value	CFP3 *eigen*			CFP6 *eigen*		
	Glass's Δ delta	Hedge's g_s	Cohen's d_s	Glass's Δ delta	Hedge's g_s	Cohen's d_s
2	1,2024	1,2638	1,2798	1,1291	1,0847	1,0985
3	1,2205	1,2725	1,2887	1,1508	1,0960	1,1100
4	1,2232	1,2744	1,2906	1,1503	1,0964	1,1103
5	1,2253	1,2778	1,2940	1,1497	1,0976	1,1116
6	1,2322	1,2852	1,3015	1,1565	1,1046	1,1186
7	1,2347	1,2877	1,3040	1,1588	1,1067	1,1208
8	1,2371	1,2900	1,3064	1,1616	1,1093	1,1234
9	1,2379	1,2913	1,3077	1,1621	1,1104	1,1245
10	1,2381	1,2915	1,3079	1,1620	1,1105	1,1246
11	1,2388	1,2922	1,3087	1,1627	1,1113	1,1254
12	1,2390	1,2924	1,3088	1,1627	1,1114	1,1255
13	1,2405	1,2939	1,3103	1,1647	1,1131	1,1272

Note: the properties of the discrete prolate spheroidal sequences (DPSS) value (2 to 13) on the effect sizes called Glass's Δ Delta, Hedges g_s and Cohen's d_s when comparing chaotic globals CFP3 and CFP6 for control subjects and those undergoing traffic noise exposure (both n=31). The remaining parameters are set as with Table 2 with the exception that Thomson's "*eigen*" nonlinear combination method to combine individual spectral estimates is applied. Again, 500 RR-intervals were used for the calculations throughout.

Table 4

The effects of discrete prolate spheroidal sequences (DPSS) value (2 to 13) on Glass's Δ Delta, Hedges g_s and Cohen's d_s

DPSS Value	CFP3 *unity*			CFP6 *unity*		
	Glass's Δ delta	Hedge's g_s	Cohen's d_s	Glass's Δ delta	Hedge's g_s	Cohen's d_s
2	1,2040	1,2647	1,2808	1,1297	1,0849	1,0987
3	1,2223	1,2736	1,2898	1,1526	1,0972	1,1112
4	1,2226	1,2735	1,2897	1,1491	1,0955	1,1094
5	1,2257	1,2782	1,2944	1,1495	1,0978	1,1118
6	1,2334	1,2864	1,3027	1,1575	1,1057	1,1198
7	1,2357	1,2887	1,3051	1,1597	1,1077	1,1218
8	1,2381	1,2911	1,3075	1,1627	1,1104	1,1246
9	1,2388	1,2922	1,3086	1,1629	1,1113	1,1254
10	1,2387	1,2922	1,3086	1,1627	1,1113	1,1254
11	1,2394	1,2929	1,3094	1,1633	1,1120	1,1261
12	1,2395	1,2929	1,3094	1,1632	1,1120	1,1262
13	1,2412	1,2946	1,3111	1,1655	1,1139	1,1281

Note: the effects of discrete prolate spheroidal sequences (DPSS) value (2 to 13) on Glass's Δ Delta, Hedges g_s and Cohen's d_s when relating chaotic globals CFP3 and CFP6 for control subjects (n=31) and those undergoing traffic noise exposure (n=31). We used 500 RR-intervals throughout. The remaining parameters are as with Table 2 and 3 with the exception that Thomson's "*unity*" nonlinear combination method to combine individual spectral estimates is applied.

Now we assess the consequence that the DPSS has on the significance of the results. We use the three effect sizes (Glass's Δ Delta, Hedges g_s and Cohen's d_s) here, as when we calculate the ANOVA1 and Kruskal-Wallis they all perform equally with $p<0,001$. Therefore, it is very difficult to distinguish which values perform best. The range of statistical outcomes is unable to discriminate between their results.

When we calculate the effect sizes the values are similar throughout with all values greater than 1,08 (large effect size) and the majority over 1,20 (very

large effect size). It is evident that the values for both CFP3 and CFP6 and for the three options of Thomson's nonlinear combination methods to combine individual spectral estimates ("adapt", "eigen" and "unity"), increase slightly with increasing DPSS. Effect sizes for CFP3 are greater and therefore more significant than CFP6. So increasing DPSS increases the significance of the results. So a DPSS of 13 where there is a reduced amount of spectral leakage and more adaptation (compared to FFT of Blackman-Tukey, DPSS of 1), is able to distinguish between the two groups in a more statistically significant manner. The mathematical markers are more efficient.

Discussion

We can recognize from the results above that the most robust parameters throughout are CFP3 and CFP6. This was the situation for all six power spectra. MTM, Welch and Periodogram did have other groups which were significant but they responded in the inappropriate manner regarding their chaotic response.

So, for three of the power spectra — Welch, MTM and Periodogram all predicated on the Fast Fourier Transform, and all are non-parametric methods. It is expected that CFP3 would be the most statistically robust parameter. It has the best values when assessed by the three effect sizes. It is notable that the Welch and MTM power spectra perform very similarly, as would be expected. A Periodogram spectrum is able to give consistent results with higher noise levels than the other two. But it is the least sophisticated algorithm that we applied in this study [12]. Despite the Periodogram matching the MTM and Welch it is rejected because, it is a blunt tool; the MTM and Welch have more parameters which can be modified to achieve better responses. The main ones we assessed are for MTM and are the DPSS (2 to 13) and Thomson's nonlinear combination methods to combine individual spectral estimates ("adapt", "eigen" and "unity").

For the other three power spectra, all are parametric methods — Burg, Covariance and Yule-Walker and the results are mostly comparable, marginally less significant when assessed by effect sizes. The order of the power spectra has little influence over the results. Here we set the orders to 16. These are more computer processor intensive algorithms, and so slower to calculate. It is recommended where possible to use the non-parametric techniques.

Returning to MTM we call these derivatives *high spectral* Entropy (*hs*Entropy) and *high spectral* Detrended Fluctuation Analysis (*hs*DFA) and they do *slightly* outperform those derived from the Welch power spectrum. Yet, the MTM power spectrum excels with regards to the various parameters which define the spectrum. For instance, the time bandwidth for the DPSS can be adjusted and Thomson's "adaptive" nonlinear combination method to combine individual spectral estimates can be attuned to the "eigenvalue" or "unity" settings.

This flexiblity enables the possibility of increasing the significance of CFP3 and CFP6 derived from MTM power spectra. It is statistically valuable to increase the DPSS to 13 and, thus outperformed those with lower DPSS when compared by the three effect sizes (see Tables 2 to 4). Adjustments of Thomson's nonlinear combinations method appears limited but "adapt" is the slightly better performer on the three effect sizes (also, Tables 2 to 4). Having time-series which are longer, and increasing the number of subjects for both control and traffic noise exposed subjects could be advantageous.

The chaotic global metrics CFP3 (and CFP6), imposed on the HRV of women exposed to traffic noises and compared to the control groups are capable of statistically discriminating the variation between them. They demonstrate an *increase* in chaotic response when comparing the controls to the traffic noise exposed group. The results are more significant for CFP3 than CFP6, and the best performers are the Welch and MTM power spectra. When the DPSS is elevated for the MTM power spectrum the mathematical marker is improved; with increased effect sizes. The MTM power spectra is advocated as the best way of calculating chaotic globals with highest DPSS set at 13. The three Thomson's nonlinear combination methods to combine individual spectral estimates settings had a minimal consequence, but the "adapt" option was slightly improved on the basis of the three effect sizes. It is accepted that longer time-series and increasing the number of subjects could be useful and, likely increase the statistical significance of the results.

Conclusion

Nonlinear HRV analysis through global chaotic approach detected changes in heart rhythm during traffic noise exposure, indicating increased nonlinear HRV during auditory stimulation.

Relationships and Activities. This study received financial support from FAPESP (Process number 2012/01366-6). Dr. Vitor E. Valenti receives financial support from the National Council for Scientific and Technological Development, an entity linked to the Ministry of Science, Technology, Innovations and Communications from Brazil (Process number 302197/2018-4).

References

1. Sim CS, Sung JH, Cheon SH, et al. The effects of different noise types on heart rate variability in men. Yonsei medical journal. 2015;56:235-43. doi:10.3349/ymj.2015.56.1.235.
2. Seely AJ, Macklem PT. Complex systems and the technology of variability analysis. Crit Care. 2004;8:R367-84. doi:10.1186/cc2948.
3. Shannon CE. A mathematical theory of communication. ACM SIGMOBILE Mobile Computing and Communications Review. 2001;5:3-55. doi:10.1145/584091.584093.
4. Peng CK, Havlin S, Stanley HE, Goldberger AL. Quantification of scaling exponents and crossover phenomena in nonstationary heartbeat time series. Chaos. 1995;5:82-7. doi:10.1063/1.166141.
5. Garner D M, Ling BW. K. Measuring and locating zones of chaos and irregularity. J Syst Sci Complex. 2014;27:494-506. doi:10.1007/s11424-014-2197-7
6. Alkan A, Kiymik MK. Comparison of AR and Welch methods in epileptic seizure detection. J Med Syst. 2006;30:413-9. doi:10.1007/s10916-005-9001-0.
7. Alkan A, Yilmaz AS. Frequency domain analysis of power system transients using Welch and Yule-Walker AR methods. Energy conversion and management. 2007;48:2129-35. doi:10.1016/j.enconman.2006.12.017.
8. Wajnsztejn R, De Carvalho TD, Garner DM, et al. Heart rate variability analysis by chaotic global techniques in children with attention deficit hyperactivity disorder. Complexity. 2016;21:412-9. doi:10.1002/cplx.21700.
9. Ghil M. The SSA-MTM Toolkit: Applications to analysis and prediction of time series. Applications of Soft Computing. 1997;3165:216-30. doi:10.1117/12.279594.
10. Subasi A. Selection of optimal AR spectral estimation method for EEG signals using Cramer-Rao bound. Comput.Biol.Med. 2007;37:183-94. doi:10.1016/j.compbiomed.2005.12.001
11. Subasi A. Application of classical and model-based spectral methods to describe the state of alertness in EEG. J Med Syst. 2005;29:473-86. doi:10.1007/s10916-005-6104-6.
12. Kiymik MK, Subasi A, Ozcalik HR. Neural networks with periodogram and autoregressive spectral analysis methods in detection of epileptic seizure. J Med Syst. 2004;28:511-22. doi:10.1023/b:joms.0000044954.85566.a9.
13. Seiver A, Daane S, Kim R. Regular low frequency cardiac output oscillations observed in critically ill surgical patients. Complexity. 1997;2;51-5.
14. Kawaguchi M, Takamatsu I, Masui K, Kazama T. Effect of landiolol on bispectral index and spectral entropy responses to tracheal intubation during propofol anaesthesia. Br.J.Anaesth. 2008;101:273-8. doi:10.1093/bja/aen162.
15. Kawaguchi M, Takamatsu I, Kazama T. Rocuronium dose-dependently suppresses the spectral entropy response to tracheal intubation during propofol anaesthesia. Br.J.Anaesth. 2009;102:667-72. doi:10.1093/bja/aep040
16. Alvarez D, Hornero R, Marcos J, et al. Spectral analysis of electroencephalogram and oximetric signals in obstructive sleep apnea diagnosis. Conf.Proc.IEEE Eng Med.Biol.Soc. 2009;2009:400-3. doi:10.1109/IEMBS.2009.5334905.
17. Banzett RB, O'Donnell CR. Should we measure dyspnoea in everyone? Eur Respir J. 2014;43:1547-50. doi:10.1183/09031936.00031114.
18. Schmidt M, Banzett RB, Raux M, et al. Unrecognized suffering in the ICU: addressing dyspnea in mechanically ventilated patients. Intensive Care Med. 2014;40:1-10. doi:10.1007/s00134-013-3117-3.
19. Goldberger AL, Peng CK, Lipsitz LA. What is physiologic complexity and how does it change with aging and disease? Neurobiol.Aging. 2002;23:23-6. doi:10.1016/S0197-4580(01)00266-4.
20. Ponnusamy A, Marques JL, Reuber M. Comparison of heart rate variability parameters during complex partial seizures and psychogenic nonepileptic seizures. Epilepsia. 2012;53:1314-21. doi:10.1111/j.1528-1167.2012.03518.x.
21. Ponnusamy A, Marques JL, Reuber M. Heart rate variability measures as biomarkers in patients with psychogenic nonepileptic seizures: potential and limitations. Epilepsy Behav. 2011;22:685-91. doi:10.1016/j.yebeh.2011.08.020.
22. Bernardo AF, Vanderlei LC, Garner DM. HRV Analysis: A Clinical and Diagnostic Tool in Chronic Obstructive Pulmonary Disease. Int Sch Res Notices. 2014;2014:673232. doi:10.1155/2014/673232.
23. Mackey MC, Milton JG. Dynamical diseases. Ann N Y Acad Sci. 1987;504:16-32. doi:10.1111/j.1749-6632.1987.tb48723.x.
24. Alves M, Garner DM, Fontes AM, et al. Linear and complex measures of heart rate variability during exposure to traffic noise in healthy women. Complexity. 2018;2018: ID 2158391. doi:10.1155/2018/2158391.
25. De Souza NM, Vanderlei LCM, Garner DM. Risk evaluation of diabetes mellitus by relation of chaotic globals to HRV. Complexity. 2015;20:84-92. doi:10.1002/cplx.21508.
26. Barreto GS, Vanderlei FM, Vanderlei LCM, Garner DM. Risk appraisal by novel chaotic globals to HRV in subjects with malnutrition. Journal of Human Growth and Development. 2014;24:243-8. doi:10.7322/jhgd.88900.
27. Vanderlei FM, Vanderlei LCM, Garner DM. Heart rate dynamics by novel chaotic globals to HRV in obese youths. Journal of Human Growth and Development. 2015;25:82-8. doi:10.7322/jhgd.96772.
28. Day BP, Evers A, Hack DE. Multipath Suppression for Continuous Wave Radar via Slepian Sequences. IEEE Transactions on Signal Processing. 2020;68:548-57. doi:10.1109/TSP.2020.2964199.
29. Razali NM, Wah YB. Power comparisons of shapiro-wilk, kolmogorov-smirnov, lilliefors and anderson-darling tests. Journal of Statistical Modeling and Analytics. 2011;2:21-33.
30. Yap BW, Sim CH. Comparisons of various types of normality tests. Journal of Statistical Computation and Simulation. 2011;81:2141-55. doi:10.1080/00949655.2010.520163.
31. Royston P. Approximating the Shapiro-Wilk W-Test for non-normality. Statistics and Computing. 1992;2:117-9.
32. Hsu JC. Multiple Comparisons: Theory and Methods. CRC Press: Boca Raton, Florida, 1996. doi:10.1201/b15074.
33. McKight PE, Najab J. Kruskal-wallis test. The corsini encyclopedia of psychology. 2010;1-1. doi:10.1002/9780470479216.corpsy0491.
34. Cohen J. Statistical power analysis for the behavioral sciences. Routledge, 2013.
35. Lakens D. Calculating and reporting effect sizes to facilitate cumulative science: a practical primer for t-tests and ANOVAs. Frontiers in psychology. 2013;4:863. doi:10.3389/fpsyg.2013.00863.
36. Hedges LV, Olkin I. Statistical methods for meta-analysis. Academic press, 2014. doi:10.2307/1164953.
37. Hedge LV. Distribution theory for Glass's estimator of effect size and related estimators. journal of Educational Statistics. 1981;6:107-28. doi:10.3102/10769986006002107.
38. Kline R. Beyond significance testing: Retorming data analyisis methods in behavioral research.(pp. 247-271). Washington, DC, US: American Psychological Association. 2004. doi:10.1037/10693-000.
39. Ialongo C. Understanding the effect size and its measures. Biochemia medica: Biochemia medica. 2016;26:150-63. doi:10.11613/BM.2016.015.
40. Sawilowsky SS. New effect size rules of thumb. Journal of Modern Applied Statistical Methods. 2009;8:26. doi:10.22237/jmasm/1257035100.
41. Thomson DJ. Spectrum estimation and harmonic analysis. Proceedings of the IEEE. 1982;70:1055-96. doi:10.1109/PROC.1982.12433.
42. Bekka RE, Chikouche D. Effect of the window length on the EMG spectral estimation through the Blackman-Tukey method. In: Seventh International Symposium on Signal Processing and Its Applications. 2003. Proceedings. IEEE. 2003; 17-20. doi:10.1109/ISSPA.2003.1224804.
43. Ahmad A, Schlindwein FS, Ng GA. Comparison of computation time for estimation of dominant frequency of atrial electrograms: Fast fourier transform, blackman tukey, autoregressive and multiple signal classification. Journal of Biomedical Science and Engineering. 2010;3:843. doi:10.4236/jbise.2010.39114.